

Impact of Leaching Operational Factors on Nickel and Manganese Recovery from Black Masses of Spent Lithium-Ion and Nickel-Metal Hydride Batteries

ARI HARDIANTO^{1,*}, DIAH N. OKTAVIA¹, ZUHROTUN NAFISAH², HERSANDY D. KUSUMA¹, FAJRIANA S. NURRUSYDA¹,
WIWIK PURWADI³, INDRA MAWARDI⁴, RANI NOPRIYANTI⁵, ADI S. ISMY⁴ and DESSY AMALIA⁶

¹Department of Chemistry, Universitas Padjadjaran, Jatinangor 45363, West Java, Indonesia

²Master Program of Environmental Science, Universitas Padjadjaran, Sumedang 45363, Indonesia

³Department of Foundry Engineering, Politeknik Manufaktur Bandung, Bandung 40135, West Java, Indonesia

⁴Department of Mechanical Engineering, Politeknik Negeri Lhokseumawe, Lhokseumawe 24301, Indonesia

⁵Department of Mechanical Engineering, Politeknik Manufaktur Bandung, Bandung 40135, West Java, Indonesia

⁶National Research and Innovation Agency, Jakarta Pusat 10340, Indonesia

*Corresponding author: E-mail: a.hardianto@unpad.ac.id

Received: 28 November 2024;

Accepted: 10 January 2025;

Published online: 31 January 2025;

AJC-21890

Spent lithium-ion (LiB) and nickel-metal hydride (NiMH) batteries pose significant environmental concerns and a valuable resource for critical metals. This study employs a two-level fractional factorial design to analyze the impact of various leaching factors on nickel and manganese recovery from a mixture of spent LiB and NiMH batteries. Results indicate that the acid concentration and liquid-to-solid ratio are the most influential factors for nickel and manganese leaching. Scanning electron microscopy analysis confirms the morphological changes in the black mass, leading to increased porosity and reduced particle size, correlating with higher metal recovery. This study provides valuable insights for developing efficient and sustainable battery recycling processes.

Keywords: Nickel, Manganese, Recycling, Spent lithium-ion and Nickel-metal hydride batteries, Sulfuric acid leaching.

INTRODUCTION

Batteries, as vital components in energy storage systems, are increasingly critical for integrating renewable energy sources like solar and wind into power grids. Additionally, in practice, batteries are predominantly used in portable applications, such as smartphones, laptops and electric vehicles, rather than large-scale grid storage. Based on Global EV outlook 2024 by mode the Stated Policies Scenario (STEPS) 2023-2035, global electric vehicle will expand to about 525 million fleet in 2035, achieving multiplication 23% annually [1]. The International Energy Agency (IEA) projects that the global electric vehicle (EV) fleet will expand to 14 million units by 2030, doubling from 7.2 million in 2021 [2].

With the escalating demand for lithium-ion batteries, a concomitant surge in spent lithium-ion batteries (LiBs) is projected. By 2030, the annual volume of LiBs waste could attain two million metric tons. A significant portion of this waste is anticipated to originate from electric vehicles, whose batteries typi-

cally have a service life of eight to ten years. As an increasing number of these vehicles reach their end-of-life, a substantial influx of battery waste is foreseen [3]. Battery waste poses significant environmental risks, including soil and water contamination, greenhouse gas emissions and biomagnification of toxic metals, which impact biodiversity and human health [4,5]. For instance, leachate from lithium-ion batteries can release harmful substances like hydrofluoric acid and hydrochloric acid, which acidify soil and facilitate the release of heavy metals, raising toxicity levels in ecosystems [6]. Additionally, the toxic metals and graphite from spent batteries contribute to dust pollution, emphasizing the urgent need for effective battery recycling in line with a circular economy [7].

Battery recycling involves several stages, including discharging, dismantling, separation and leaching. Hydrometallurgy is a promising technology for sustainable battery recycling compared to pyrometallurgical methods [8], potentially result in significant loss of valuable metals and generate harmful gas emissions [9]. The correct choice of acid solvent in leaching

processes is essential for a successful metal extraction process [10]. Hydrochloric acid (HCl) produces chloride based by-products and high corrosiveness necessitate specific wastewater treatments and corrosion-resistant equipment [11]. In addition, nitric acid (HNO₃) often considered too aggressive due to the production of nitrogen oxides (NO_x), which require stringent emission controls [12,13].

Sulfuric acid (H₂SO₄) is a commonly used solvent due to its high leaching efficiency. This process often involves the reduction of metal oxides or other compounds, facilitated by the presence of sulfuric acid and sometimes additional reductants [9]. Reducing agents are essential for converting higher valency metal oxides into their lower valency states, which are more soluble in acidic solutions. This conversion is critical for the effective leaching of metals like manganese, cobalt and nickels [14]. Some examples of reductants that are commonly used include sodium bisulfite (NaHSO₃), ascorbic acid (C₆H₈O₆) and hydrogen peroxide (H₂O₂) [15]. While the addition of reductants can enhance the dissolution of certain materials, it introduces a trade-off between process efficiency and overall sustainability, as it necessitates the introduction of additional chemicals into the recycling stream. Moreover, the recycling of spent LiBs by hydrometallurgical methods is hindered by the generation of high-Na-low-Li sulfate raffinate after metal recovery. Conventional methods, such as neutralization, precipitation and solvent extraction, leave a Li-rich raffinate, which can be further processed to recover Li. However, these processes introduce significant amounts of sodium, resulting in the production of large quantities of low-value sodium sulfate by-products. Consequently, a reductant that doubles as a hydrogen storage material is necessary. nickel-metal hydride (NiMH) batteries exemplify this property, as their composition—a blend of rare earth metals (La, Ce, Pr and Nd), nickel, cobalt and manganese—forms an alloy with a pronounced ability to absorb hydrogen [9].

While Liu *et al.* [9] provided compelling evidence of the synergistic benefits of combining Li-ion (LiB) and nickel-metal hydride (NiMH) batteries, their methodology primarily relied on a univariate approach. This valuable approach neglected the comparative effects and complex interactions between various parameters influencing recovery performance [16]. The parameters include sulfuric acid concentration, reaction temperature, liquid-to-solid ratio, the ratio of LiB to NiMH and the timing of NiMH addition. Therefore, we adopted a multivariate experimental design, *i.e.* two-level fractional factorial design [16] to comparative effects and complex interactions between various parameters influencing recovery performance of nickel and manganese from spent battery black mass. A series of experiments were conducted by varying parameters. This comprehensive approach facilitates the identification of crucial parameters for a thorough exploration of the experimental space to seek optimal nickel and manganese leaching conditions.

EXPERIMENTAL

Spent lithium-ion batteries (LiBs) and nickel-metal hydride (NiMH) batteries were obtained from the local recycling facilities. Technical-grade sulfuric acid (Bratachem, Indonesia)

was used as the leaching agent to simulate the industrial-scale processing. Demineralized water was employed for dilution purpose. Manganese and nickel standard solutions traceable to standard reference materials (SRM) from NIST were purchased from Merck.

Discharging and manual dismantling of spent batteries:

To ensure safe handling, each battery was fully discharged prior to dismantling using an *ex situ* method, adapted from Ojanen *et al.* [17] with a modification. After being fully discharged, each battery was manually dismantled to separate and isolate the black mass just the component containing the mixed metal oxides along with all the other valuable elements. Henceforth, the terms “LiB” and “NiMH” will be used to refer to the black mass components of lithium-ion and nickel-metal hydride batteries, respectively. Processing stages for black mass recovery from batteries involves manual dismantling with great care using hand tools, such as screwdrivers, pliers and scalpels, in a way that did not damage the internal components when the battery casings are disassembled. First, the casings were pried open to access the internal layers, including the anode, cathode, electrolyte and separator. Every component was carefully removed manually, isolating the black mass material from the rest of the battery to prevent contamination. Isolated black mass material was collected and separately stored in sealed containers to protect it from atmospheric moisture and oxidation before the leaching phase.

Leaching optimization and experimental design: Black mass leaching using sulfuric acid was adapted from Liu *et al.* [9]. The effects of six parameters—the concentration of sulfuric acid, leaching temperature (T), liquid-to-solid ratio (L/S), the mass ratio of LiB-to-NiMH (LiB/NiMH), total leaching time (t_{leaching}) and the time of NiMH addition ($t_{\text{add NiMH}}$)—on manganese and nickel leaching recoveries were investigated. The experimental design was based on a two-level fractional factorial approach [16,18] that studied main and binary interactions among these parameters, leading to a total number of 16 experiments. Two sulfuric acid concentrations, 0.5 M and 3 M, were studied to determine the effect of acid strength on the dissolution efficiency of the black mass. Temperature was controlled at two levels: room temperature and 70 °C, allowing an insight into how the thermal conditions impact the leaching kinetics and metal recovery.

The L/S, expressed as the volume of sulfuric acid per unit mass of black mass, was varied at 8:1 and 11:1 to identify the amount of acid needed for the most efficient leaching. The composition of the black material was additionally modified by adjusting the LiB/NiMH ratio to two levels, 0.25:1 and 0.75:1, to examine the impact of varying battery type proportions on the leaching process. Leaching duration was also varied to determine whether a longer exposure time could improve the metal recovery rate, with two total times of 90 min and 120 min. The timing of NiMH addition was established at two different intervals *viz.* 30 min and 60 min following the initiation of the leaching process, facilitating the evaluation of the effects of staged addition on metal recovery. Table-1 lists the parameter combinations for each of a two-level fractional factorial consisting of 16 experiment runs. For instance, experiment 1 was cond-

TABLE-1

TWO-LEVEL FRACTIONAL FACTORIAL DESIGN IN STUDYING THE EFFECTS OF PARAMETERS IN NICKEL AND MANGANESE LEACHING FROM THE BLACK MASSES OF SPENT LiB AND NiMH BATTERIES. THE FACTORS INCLUDE THE CONCENTRATION OF SULFURIC ACID ($[H_2SO_4]$), LEACHING TEMPERATURE (T), LIQUID-TO-SOLID RATIO (L/S), THE MASS RATIO OF LiB-to-NiMH (LiB/NiMH), TOTAL LEACHING TIME ($t_{leaching}$) AND THE TIME OF NiMH ADDITION ($t_{add NiMH}$). THE VALUE 0.25 IN LiB/NiMH MEANS 0.25 PART FOR LiB AND 1 PART FOR NiMH AND LIKewise FOR 0.75

No.	$[H_2SO_4]$ (M)	Temp. ($^{\circ}C$)	Liquid/solid	LiB/NiMH	$t_{leaching}$ (min)	$t_{add NiMH}$ (min)
1	0.5	27	8	0.75	90	60
2	3.0	70	8	0.25	90	30
3	0.5	70	11	0.25	90	60
4	0.5	27	8	0.25	90	30
5	3.0	27	8	0.25	120	60
6	3.0	27	11	0.75	90	30
7	3.0	70	8	0.75	90	60
8	0.5	70	8	0.25	120	60
9	0.5	27	11	0.75	120	60
10	0.5	27	11	0.25	120	30
11	0.5	70	8	0.75	120	30
12	3.0	27	8	0.75	120	30
13	3.0	27	11	0.25	90	60
14	0.5	70	11	0.75	90	30
15	3.0	70	11	0.75	120	60
16	3.0	70	11	0.75	120	30

ucted with 0.5 M sulfuric acid at room temperature, an L/S ratio of 8:1, a LiB/NiMH of 0.75:1, a total leaching time of 90 min and NiMH addition after 60 min.

Detection method: Black mass before leaching was characterized by using X-ray fluorescence spectrometer (XRF, Rigaku Supermini200, Japan). The black mass before leaching and the representative black mass after leaching were also characterized by using scanning electron microscope (SEM, COXEM EM-30N, Japan) instrument. The concentrations of manganese and nickel in leaching solution were determined by flame atomic absorption spectrometer (Shimadzu AA-7000F, Japan) instrument.

RESULTS AND DISCUSSION

Nickel leaching: After conducting the experimental runs as listed in Table-1, nickel and manganese concentrations in the resulting leachates were determined by using ICP-OES. Nickel and manganese recoveries were computed according to XRF results (Table-2). The resulting values of nickel recovery were analyzed and presented as main effect plots (Fig. 1). The plot illustrates how each factor influences nickel leaching recovery from LiB and NiMH spent batteries. As observed in Fig. 1, most factors exhibit positive correlations with Ni leaching recovery. Specifically, increasing the concentration of sulfuric acid, L/S,

LiB/NiMH, leaching temperature and leaching duration positively affects nickel recovery. However, the time of NiMH black mass addition shows an inverse effect, where earlier addition leads to higher recovery, suggesting that the timing of introducing NiMH impacts the overall process dynamics.

Subsequently, an analysis of variance with a 95% confidence level was performed to determine which factors significantly affect nickel leaching recovery. As shown in Table-3, the concentration of sulfuric acid and the L/S have statistically significant effects on nickel recovery, with p -values of 0.000130 and 0.000552, respectively. The use of 3 M sulfuric acid significantly increases Ni leaching recovery compared to 0.5 M, with a highly significant p -value of 0.000130. This analysis result was expected since the presence of H^+ ions help to dissolve nickel compounds by breaking down metal oxides and hydroxides, facilitating the release of Ni^{2+} into the solution [19,20]. Furthermore, sulfate (SO_4^{2-}) ions enhance nickel solubility by forming soluble complexes with nickel ions, resulting in nickel sulfate, which remain dissolved in water [21]. This complexation prevents the precipitation of nickel ions and stabilizes them in the solution. The presence of sulfate ions also increases the reaction rate of nickel ion entry into the solution [22]. Their combined action develops a reactive medium that promotes nickel dissolution.

TABLE-2

PERCENTAGE (w/w) OF ELEMENTS CONTAINED IN THE BLACK MASSES OF LiB AND NiMH. ELEMENTAL COMPOSITION IN THE BLACK MASSES WAS DETERMINED BY USING XRF

Element	Percentage w/w (%)		Element	Percentage w/w (%)		Element	Percentage w/w (%)		Element	Percentage w/w (%)	
	LiB	NiMH		LiB	NiMH		LiB	NiMH		LiB	NiMH
Al	0.54	0.67	Cu	2.32	0.10	Na	0.00	0.00	S	0.08	0.03
Ag	0.00	0.00	F	0.00	0.00	Nb	0.06	0.05	Si	0.26	0.14
Cd	0.00	1.31	Fe	0.71	0.19	Nd	0.00	0.60	Sm	0.00	0.00
Ce	0.00	1.67	K	0.10	0.61	Ni	19.56	59.15	Y	0.00	0.26
Cl	0.09	0.05	La	0.00	3.35	P	0.59	0.00	Zn	0.00	3.46
Co	21.90	5.27	Mg	0.06	0.00	Pr	0.00	0.17			
Cr	0.09	0.00	Mn	28.89	1.28	Rh	0.52	0.00			

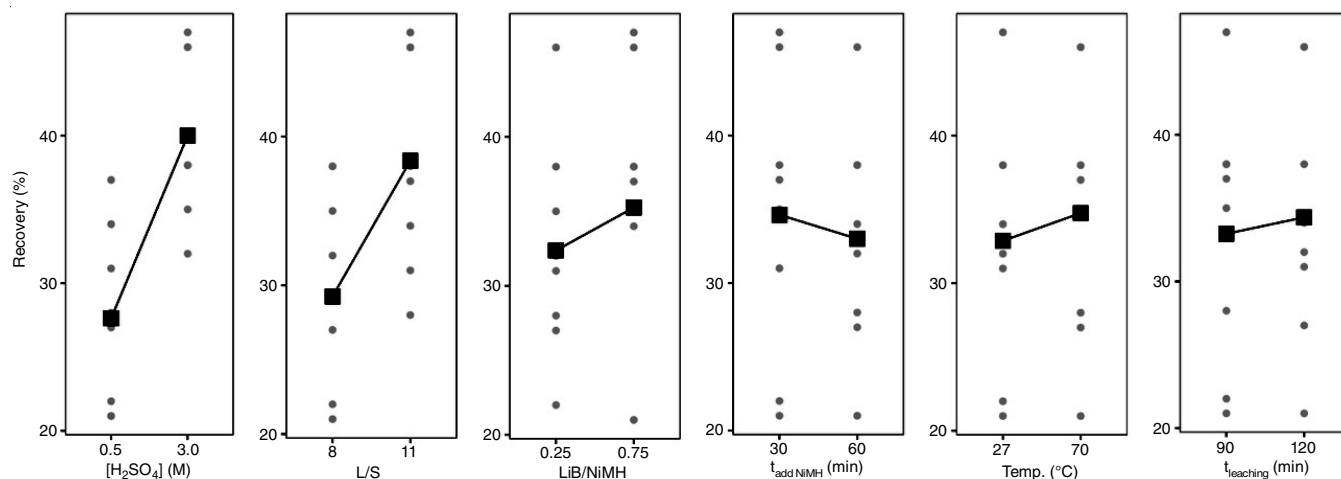


Fig. 1. Main effect plots of several factors in the nickel leaching from black mass mixture of LiB and NiMH spent batteries. The factors include the concentration of sulfuric acid ($[H_2SO_4]$), leaching temperature (T), liquid-to-solid ratio (L/S), the mass ratio of LiB-to-NiMH ($LiB/NiMH$), total leaching time ($t_{leaching}$) and the time of NiMH addition ($t_{add NiMH}$). The value 0.25 in $LiB/NiMH$ means 0.25 part for LiB and 1 part for NiMH and likewise for 0.75. The black squares represent mean values, whereas grey points are the individual data

TABLE-3
ANALYSIS OF VARIANCE FOR THE MULTIFACTOR EFFECTS ON NICKEL LEACHING RECOVERY FROM BLACK MASS MIXTURE OF LiB AND NiMH SPENT BATTERIES

	df	Sum square	Mean square	F value	p-value
$[H_2SO_4]$	1	612.6	612.6	112.14	0.000130
L/S	1	333.1	333.1	60.973	0.000552
$LiB/NiMH$	1	33.1	33.1	6.053	0.057214
$t_{add NiMH}$	1	10.6	10.6	1.934	0.223078
Temp.	1	14.1	14.1	2.574	0.169513
$t_{leaching}$	1	5.1	5.1	0.927	0.379917
$[H_2SO_4] \times LiB/NiMH$	1	10.6	10.6	1.934	0.223078
$[H_2SO_4] \times t_{add NiMH}$	1	7.6	7.6	1.384	0.292307
$L/S \times LiB/NiMH$	1	22.6	22.6	4.13	0.097818
$L/S \times t_{add NiMH}$	1	18.1	18.1	3.307	0.128671
Residuals	5	27.3	5.5		
Adjusted R^2		0.9251			

The significantly higher nickel leaching recoveries at a L/S of 8 compared to 2 (p -value of 0.000552) can be attributed to several factors related to the leaching process dynamics. A higher L/S generally enhances the leaching efficiency by increasing the availability of the leaching agent, which in this case is sulfuric acid, to interact with the solid particles. The high availability of the leaching agent facilitates the dissolution of nickel from the battery materials into the solution [22]. Moreover, the higher volume of leaching solution helps maintain a lower concentration of nickel ions in the solution, which can enhance the driving force for the leaching reaction according to Le Chatelier's principle [23]. Furthermore, a higher L/S can improve the mass transfer conditions, reducing the diffusion limitations that might otherwise hinder the leaching process [24].

We considered $LiB/NiMH$ as operational factor in current study since their mixture reported to have a synergistic leaching effect [9]. The results show that a $LiB/NiMH$ of 0.75:1 yields higher nickel recovery than that of 0.25:1, showing the synergistic effect a synergistic effect between the two battery types [9]. However, within these levels, $LiB/NiMH$ does not significantly affect nickel recovery (Table-3). This result may be because

the leaching process is more dependent on the chemical interactions facilitated by the leaching agent, such as sulfuric acid [25], rather than $LiB/NiMH$.

Meanwhile, the timing of NiMH addition exhibits a unique inverse effect, with earlier addition leading to better recovery. This earlier introduction allows for a longer remaining leaching time, potentially facilitating equilibrium. However, this effect is not statistically significant at the current levels of 30 and 60 min. Similarly, leaching time in the present study, with levels of 90 and 120 min, does not significantly affect nickel leaching recovery. This phenomenon may be due to the leaching process reaching equilibrium quickly. Investigations into the leaching kinetics of nickel from various sources, including spent catalysts and lateritic ores, have found that extending leaching time beyond a certain threshold does not substantially increase nickel recovery [26]. The non-significant effect of temperature in present study is in line with another study [26]. Studies on nickel leaching from lateritic ores have demonstrated that temperature variations within certain ranges do not significantly impact leaching efficiency. Similarly, study on spent catalysts indicates that temperature changes have minimal effect on the nickel extraction rates [27].

Manganese leaching: The effects of most factors on the manganese leaching were comparable to those on Ni leaching, except for temperature (Fig. 2). Temperature exhibits a slight negative correlation with Mn leaching recovery at 27 and 70 °C, but not statistically significant (Table-4). Analysis of variance (Table-4) reveals that sulfuric acid concentration and L/S are the most significant factors influencing manganese leaching recovery, with *p*-values of 0.000235 and 0.001304, respectively. The LiB/NiMH and leaching duration are also statistically significant at a 95% confidence level, with *p*-values of 0.018438 and 0.034749.

Interestingly, at a 90% confidence level, two-factor interactions between sulfuric acid concentration and temperature, as well as sulfuric acid concentration and LiB/NiMH, are statistically significant. Both interactions positively affect Mn leaching recovery, indicating that increasing sulfuric acid concentration and temperature or sulfuric acid concentration and LiB/NiMH collectively enhances manganese leaching. This analysis emphasizes the importance of considering interactions when optimizing leaching processes, particularly the interdependent effect of sulfuric acid concentration and LiB/NiMH with a *p*-value of 0.052775.

Morphological studies: Scanning electron microscopy (SEM) was conducted to visualize the morphological changes

of the black mass materials before and after leaching. Fig. 3a-b depict the morphology of LiB and NiMH black masses, respectively, prior to leaching. Fig. 3c represents the black mass mixture after leaching under conditions that resulted in the lowest leaching recovery, while Fig. 3d shows the mixture after leaching under conditions that yielded the highest recovery.

The LiB black mass (Fig. 3a) exhibits a relatively uniform particle size distribution, with particles appearing spherical or slightly irregular in shape. The NiMH black mass (Fig. 3b) shows a more heterogeneous morphology, with a wider range of particle sizes and shapes. Some particles appear more irregular compared to those in the LiB black mass. Moreover, the NiMH black mass exhibits a more porous and dusty appearance, which is likely due to the presence of fine particles and internal voids. The black mass after leaching under a condition with low recovery (Fig. 3c) shows a more porous structure. This suggests that the leaching process has effectively dissolved and removed certain components from the black mass. However, some undissolved particles are still visible, indicating incomplete leaching. The black mass after leaching under a condition with high recovery (Fig. 3d) appears to have more altered morphology compared to Fig. 3c. The particles are even more porous, suggesting more complete dissolution of the metal components. There are fewer visible undissolved particles indicating that the leaching

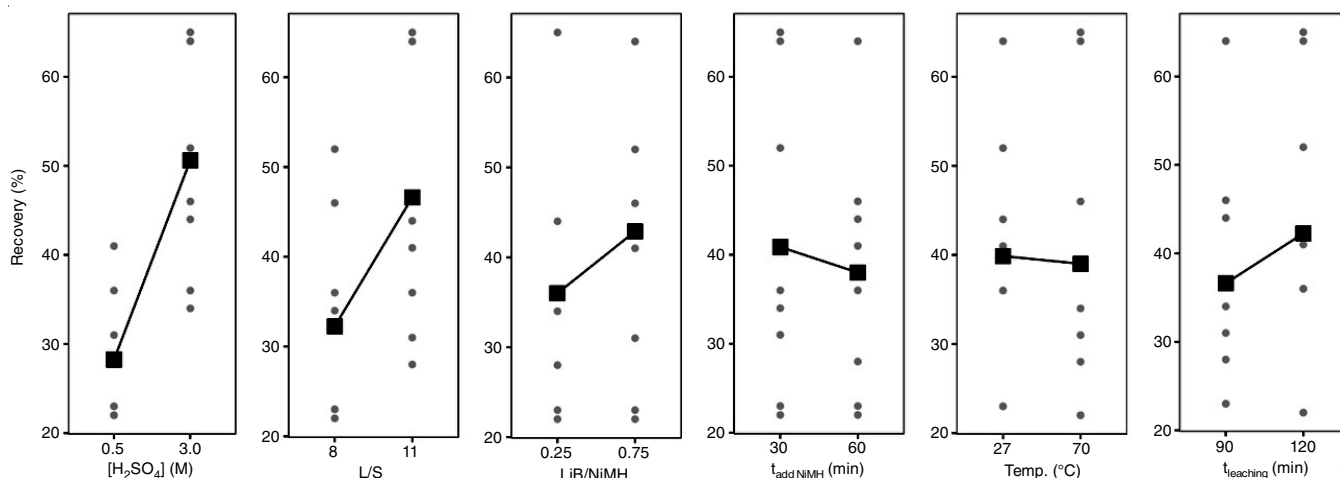


Fig. 2. Main effect plot of several factors in the manganese leaching from black mass mixture of LiB and NiMH spent batteries

TABLE-4
ANALYSIS OF VARIANCE FOR THE MULTIFACTOR EFFECTS ON MANGANESE LEACHING RECOVERY FROM BLACK MASS MIXTURE OF LiB AND NiMH SPENT BATTERIES

	df	Sum square	Mean square	F value	p-value
[H ₂ SO ₄]	1	0.20026	0.20026	156	0.000235
Temp.	1	0.00031	0.00031	0.239	0.650507
L/S	1	0.08266	0.08266	65	0.001304
LiB/NiMH	1	0.01891	0.01891	15	0.018438
t _{leaching}	1	0.01266	0.01266	10	0.034749
t _{add NiMH}	1	0.00331	0.00331	3	0.183463
[H ₂ SO ₄] × Temp.	1	0.00681	0.00681	5	0.082501
[H ₂ SO ₄] × L/S	1	0.00331	0.00331	3	0.183463
[H ₂ SO ₄] × LiB/NiMH	1	0.00951	0.00951	7	0.052775
[H ₂ SO ₄] × t _{add NiMH}	1	0.00456	0.00456	4	0.132397
L/S × t _{add NiMH}	1	0.00141	0.00141	1	0.353930
Residuals	4	0.00512	0.00128		
Adjusted R ²		0.9449			

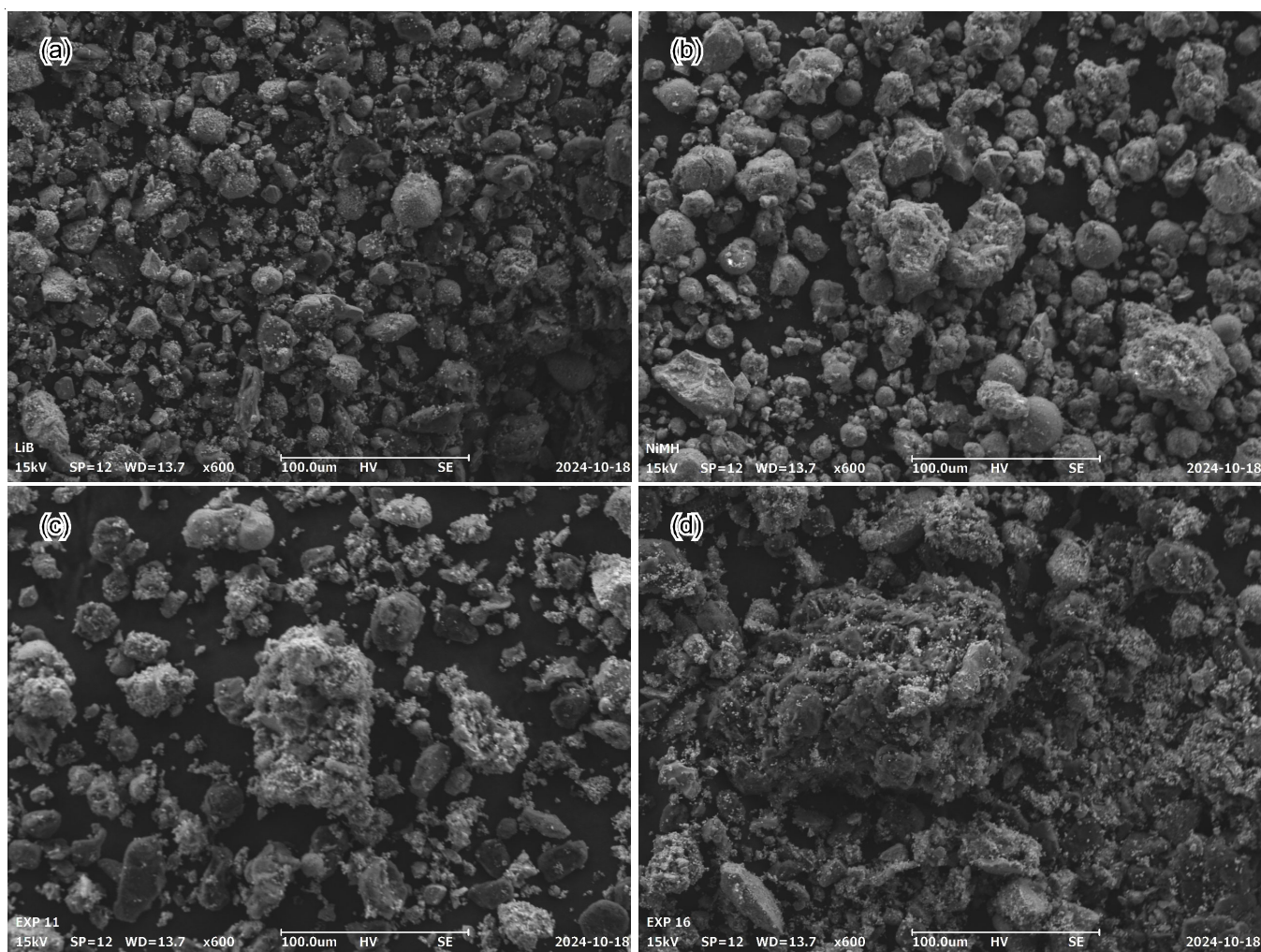


Fig. 3. Scanning electron microscopy (SEM) images of black mass materials: (a) LiB black mass, (b) NiMH black mass, (c) LiB-NiMH mixture after leaching under a condition yielding low recovery and (d) LiB-NiMH mixture after leaching under a condition yielding high recovery

process was more effective in extracting the manganese and nickel.

Conclusion

This study investigated the influence of various factors on nickel and manganese recovery from the synergistic leaching of the black masses of spent lithium-ion (LiB) and nickel-metal hydride (NiMH) batteries. A two-level fractional factorial design was employed to evaluate the influence of the factors, including sulfuric acid concentration, temperature, liquid-to-solid ratio, LiB/NiMH ratio, leaching duration and the time of NiMH addition. The results revealed that sulfuric acid concentration and liquid-to-solid ratio are the most significant factors affecting both nickel and manganese leaching. Higher acid concentrations and liquid-to-solid ratios may promote metal dissolution by increasing the availability of H^+ ions and improving mass transfer, respectively. The LiB/NiMH ratio and leaching time also significantly influence manganese leaching indicating that the synergistic effect between the two battery types can enhance manganese recovery. The timing of NiMH addition has an inverse effect on nickel leaching, with earlier addition leading to higher

recovery. This suggests that the initial dissolution of NiMH components can generate favourable conditions for subsequent nickel leaching from LiB. Meanwhile, SEM analysis provided insights into the morphological changes of the black mass during the leaching process. The observed reduction in particle size and increased porosity after leaching were correlated with higher metal recoveries. Overall, this study provides valuable insights into the factors affecting nickel and manganese recovery from the synergistic leaching of LiB and NiMH spent batteries. These findings can be used to optimize the leaching process and maximize the recovery of valuable metals. Future research could explore the recovery of other valuable metals, such as cobalt and lithium, from the leachate to further enhance the economic viability of the recycling process.

ACKNOWLEDGEMENTS

The authors gratefully acknowledge APTV for providing the Mandatory Research Program Grant for the Development of Electric Batteries at PTV, under Decree No. 28/D4/O/2024 and Contract No. 115/SPK/D.D4/PPK.01.APTV/IV/2024.

CONFLICT OF INTEREST

The authors declare that there is no conflict of interests regarding the publication of this article.

REFERENCES

- International Energy Agency, Renewables 2023, Paris (2024); https://iea.blob.core.windows.net/assets/96d66a8b-d502-476b-ba94-54ffda84cf72/Renewables_2023.pdf
- International Energy Agency, Global EV Outlook 2024, IEA, Paris, (2024); <https://iea.blob.core.windows.net/assets/a9e3544b-0b12-4e15-b407-65f5c8ce1b5f/GlobalEVO Outlook2024.pdf>
- S.S. Sharma and A. Manthiram, *Energy Environ. Sci.*, **13**, 4087 (2020); <https://doi.org/10.1039/D0EE02511A>
- B. Jiang, A. Adebayo, J. Jia, Y. Xing, S. Deng, L. Guo, Y. Liang and D. Zhang, *J. Hazard. Mater.*, **362**, 187 (2019); <https://doi.org/10.1016/j.jhazmat.2018.08.060>
- D.K. Gupta, A. Iyer, A. Mitra, S. Chatterjee and S. Murugan, 2024, preprint, <https://doi.org/10.21203/rs.3.rs-3730110/v1>
- A. Boyden, V.K. Soo and M. Doolan, *Procedia CIRP*, **48**, 188 (2016); <https://doi.org/10.1016/j.procir.2016.03.100>
- D.H.P. Kang, M. Chen and O.A. Ogunseitan, *Environ. Sci. Technol.*, **47**, 5495 (2013); <https://doi.org/10.1021/es400614y>
- S. Srinivasan, S. Shanthakumar and B. Ashok, *Energy Rep.*, **13**, 789 (2025); <https://doi.org/10.1016/j.egyr.2024.12.043>
- F. Liu, C. Peng, A. Porvali, Z. Wang, B.P. Wilson and M. Lundström, *ACS Sustain. Chem. & Eng.*, **7**, 16103 (2019); <https://doi.org/10.1021/acssuschemeng.9b02863>
- S. Kursunoglu, N. Kursunoglu, S. Hussaini and M. Kaya, *J. Clean. Prod.*, **283**, 124659 (2021); <https://doi.org/10.1016/j.jclepro.2020.124659>
- A.-F. Yi, Z.-W. Zhu, Y.-H. Liu, J. Zhang, H. Su and T. Qi, *Rare Met.*, **40**, 1971 (2021); <https://doi.org/10.1007/s12598-020-01503-4>
- H. Chen, S. Gu, Y. Guo, X. Dai, L. Zeng, K. Wang, C. He, G. Dodbiba, Y. Wei and T. Fujita, *Hydrometallurgy*, **205**, 105746 (2021); <https://doi.org/10.1016/j.hydromet.2021.105746>
- R. Yuliusman, R. Fajaryanto, A. Nurqomariah and Silvia, *E3S Web Conf.*, **67**, 03025 (2018); <https://doi.org/10.1051/e3sconf/20186703025>
- A.R.F. Carreira, A.F.M. Nogueira, I.L.D. Rocha, F. Sosa, A.M. Da Costa Lopes, H. Passos, N. Schaeffer and J.A.P. Coutinho, *ChemSusChem*, **17**, e202301801 (2024); <https://doi.org/10.1002/cssc.202301801>
- L.-P. He, S.-Y. Sun, Y.-Y. Mu, X.-F. Song and J.-G. Yu, *ACS Sustain. Chem. & Eng.*, **5**, 714 (2017); <https://doi.org/10.1021/acssuschemeng.6b02056>
- D.C. Montgomery, Design and Analysis of Experiments, John Wiley & Sons, Inc., Tempe, Arizona, USA, edn. 10 (2019).
- S. Ojanen, M. Lundström, A. Santasalo-Aarnio and R. Serna-Guerrero, *Waste Manag.*, **76**, 242 (2018); <https://doi.org/10.1016/j.wasman.2018.03.045>
- M. Abidin, M. Yusuf, W. Widayat, T. Subroto, N. Nurainy and A. Hardianto, *Trends Sci.*, **21**, 7142 (2023); <https://doi.org/10.48048/tis.2024.7142>
- J. Wen and M.S. Lee, *J. Chem. Technol. Biotechnol.*, **98**, 2841 (2023); <https://doi.org/10.1002/jctb.7490>
- Y. Wang, W. Qin and J. Han, *Miner. Eng.*, **207**, 108577 (2024); <https://doi.org/10.1016/j.mineng.2024.108577>
- M.A. Deyab, M.M. Alghamdi and A.A. El-Zahhar, *Sci. Rep.*, **14**, 1853 (2024); <https://doi.org/10.1038/s41598-024-52281-3>
- A.M.A.-A. Otron, T. Millogo, L.-H. Tran and J.-F. Blais, *Environ. Technol.*, **45**, 4156 (2024); <https://doi.org/10.1080/09593330.2023.2243391>
- I.B. Illés and T. Kékesi, *Miner. Eng.*, **201**, 108169 (2023); <https://doi.org/10.1016/j.mineng.2023.108169>
- X. Peng, L. Shi, T. Qu, Z. Yang, L. Lin, G. Xie and B. Xu, *Separations*, **10**, 64 (2023); <https://doi.org/10.3390/separations10020064>
- A.R.F. Carreira, A. Nogueira, A.P.S. Crema, H. Passos, N. Schaeffer and J.A.P. Coutinho, *Chem. Eng. J.*, **475**, 146374 (2023); <https://doi.org/10.1016/j.cej.2023.146374>
- P.P.M. Ribeiro, I.D. dos Santos, R. Neumann, A. Fernandes and A.J.B. Dutra, *Metall. Mater. Trans., B, Process Metall. Mater. Proc. Sci.*, **52**, 1739 (2021); <https://doi.org/10.1007/s11663-021-02141-6>
- S. İlhan and D. Akgün, *J. Sustain. Metall.*, **7**, 470 (2021); <https://doi.org/10.1007/s40831-021-00351-5>